Supplemental Online Material

Model description

CASA model

CASA is a classic light use efficiency model that utilises satellite measurements to estimate vegetation net primary production (Potter et al., 1993). It directly translates radiation into Net Primary Production (NPP) based on the notion of light use efficiency (LUE), which is a product of optimal efficiency and the regulatory functions of environmental factors (e.g., temperature and water stress). The complete expression for NPP in the CASA is thus given by:

$$NPP = PAR \times fPAR \times LUE_{\max} \times T_{s1} \times T_{s2} \times W_s \quad (1)$$

where *PAR* is the incident photosynthetically active radiation per time period, *fPAR* is the fraction of *PAR* absorbed by the vegetation canopy, LUE_{max} is the potential *LUE* (g C m^{-2} MJ^{-1} APAR) without environment stress, T_{s1} and T_{s2} are two downward-regulation scalars for the effects of temperature, W_s is the downward-regulation scalar for the effects of moisture on *LUE* of vegetation.

fPAR is calculated as a linear function of the simple ratio (*SR*) according to Sellers et al. (1993),

$$fPAR = \min\{SR / (SR_{\max} - SR_{\min}) - SR_{\min} / (SR_{\max} - SR_{\min}), 0.95\} \quad (2)$$

$$SR = (1 + NDVI) / (1 - NDVI) \quad (3)$$

where SR_{min} represents *SR* for unvegetated land areas and is set to 1.08 for all grid cells. SR_{max} approximates the value at which all downwelling solar radiation is intercepted and corrects for effects of canopy architecture and residual cloud contamination. NDVI is Normalized Difference Vegetation Index.

T_{s1} serves to depress LUE_{max} at very high and very low temperatures (T_{s1}) and to depress LUE_{max} when the temperature is above or below the optimum temperature (T_{opt}), where T_{opt} is defined as the air temperature in the month when the NDVI reaches its maximum for the year. T_{s2} reflects the concept that the efficiency to light utilization should be depressed when plants are growing at temperatures displaced from their optimum, has an asymmetric bell shape that falls off more quickly at high than at low temperature. W_s represents water stress on light use efficiency using actual ecosystem evapotranspiration (ET) and potential evapotranspiration (PET). T_{s1}, T_{s2} and W_s are calculated as the following equations.

$$T_{s1} = 0.8 + 0.02 \times T_{opt} - 0.0005 \times T_{opt} \times T_{opt} \quad (4)$$

$$T_{s2} = 1.1919 / \{1 + e^{[0.2(T_{opt} - 10 - T)]}\} / \{1 + e^{[0.3(-T_{opt} - 10 + T)]}\} \quad (5)$$

$$W_{\varepsilon} = 0.5 + 0.5 \times (ET / PET) \quad (6)$$

CASA model simulates directly NPP, and an approximate conversion of 0.5 between NPP and GPP is used in this study.

CFix model

C-Fix is a light use efficiency type parametric model driven by temperature (T), PAR and fPAR (Veroustraete et al., 2002). The model uses the following equations to estimate vegetation GPP on a daily basis:

$$GPP = PAR \times fPAR \times LUE_{wl} \times \rho(T) \times CO_2 fert \quad (7)$$

where LUE_{wl} is light use efficiency by considering the impact of water stress. $\rho(T)$ is the normalised temperature dependency factor, defined according to Veroustraete et al. (1994); $CO_2 fert$ is the normalised CO_2 fertilisation factor, defined according to Veroustraete et al. (1994).

Verstraeten et al. (2006) integrated the impact of water limitation on light use efficiency by considering two stomatal regulating factors from soil moisture deficit (F_s) and atmospheric changes (F_a), which were simulated by soil moisture and evaporative fraction (*EF*) respectively. Due to the difficulties at regional simulations of soil moisture, we only consider the impacts of atmospheric changes on *LUE* in this study, and simplified the regulation equation of water limitation as following.

$$LUE_{wl} = (LUE_{\min} + F_a \times (LUE_{\max} - LUE_{\min})) \quad (8)$$

where LUE_{wl} was delimited between a maximum (LUE_{max}) and minimum value (LUE_{min}) (g C MJ^{-1} APAR).

CFix model uses a linear equation to describe the relationship between *fPAR* and NDVI, and uses a set of empirical constants according to Myneni and Williams (1994):

$$fPAR = 0.8624 \times NDVI - 0.0814 \quad (9)$$

The temperature dependency factor *p(T)* is described by Wang (1996). CO_2 fertilisation equation was defined by Veroustraete (1994) as the increase in carbon assimilation due to CO_2 levels above the atmospheric background level (or reference level).

$$\rho(T) = \frac{e^{(C_l - \frac{\Delta H_{a,P}}{R_g \times T})}}{1 + e^{(\frac{\Delta S \times T - \Delta H_{d,P}}{R_g \times T})}} \quad (10)$$

$$CO_2\,fert = \frac{[CO_2] - \frac{[O_2]}{2s}}{[CO_2]^{ref} - \frac{[O_2]}{2s}} \frac{K_m \times (1 + \frac{[O_2]}{K_0}) + [CO_2]^{ref}}{K_m \times (1 + \frac{[O_2]}{K_0}) + [CO_2]} \quad (11)$$

where C_l, ΔS, $\Delta H_{a,P}$, $\Delta H_{d,P}$, R_g at the temperature response equation are 21.77, 704.98 J K^{-1} mol^{-1}, 52750 J mol^{-1}, 211000 J mol^{-1}, 8.31 J K^{-1} mol^{-1} according to Veroustraete et al. (2002); the parameter values of *s*, K_m, K_o, $[CO_2]^{ref}$ are 2550, 948, 30 and 281 ppm respectively. In this study,

$[O_2]$ was set to 209000 ppm, and $[CO_2]$ was set to be annual mean global carbon dioxide concentration using measurements of weekly air samples from the Cooperative Global Air Sampling network (http://www.esrl.noaa.gov/gmd/ccgg/trends/global.html)

CFlux model

The carbon flux model (CFlux) integrates data from multiple sources (Turner et al., 2006; King et al., 2011), and model inputs include daily meteorological data and satellite-derived information on land cover, stand age and MODIS-fPAR product. A unique feature for CFlux model is that GPP is influenced by stand age. The model can be represented as the following equations:

$$GPP = PAR \times fPAR \times LUE_{eg} \quad (12)$$

$$LUE_{eg} = LUE_{g\_base} \times T_s \times \min(W_s, S_{SWg}) \times S_{SAg} \quad (13)$$

$$LUE_{base} = (LUE_{\max} - LUE_{cs}) \times S_{CI} + LUE_{cs} \quad (14)$$

The scalars for minimum temperature (T_s) and vapour pressure deficit (W_s) are formulated as in MODIS-GPP product (i.e. equation (20, 21)) with a linear ramp (1 to 0) between a value when the influence is at a minimum and a value when it is at a maximum (i.e. when LUE is reduced to 0). The scalar for the influence of soil water (S_{SWg}) is based on the ratio of current soil water content to soil water holding capacity (*WHC*). When the ratio is above a value of 0.5, S_{SWg} is set to 1.0 (no influence) and below a ratio of 0.5 there is a linear ramp from S_{SWg} of 1 to an S_{SWg} of 0 as the ratio hits 0. We simplified the simulations of soil moisture and used evaporative fraction (*EF*) to indicate S_{SWg}. In the case of forest cover types, a scalar for the effect of stand age on GPP (S_{SAg}) is implemented to reflect observations of reduced vegetation production in older stands (Van Tuyl et

al., 2005). S_{CI} cloudiness index scalar that varies from 0 on clear days to 1 on fully overcast days and is inferred from the ratio of PAR to potential PAR (Turner et al., 2006). LUE_{cs} is initial *LUE* for clear sky days. LUE_{max} is initial *LUE* for overcast days. The age scalar (S_{Sag}) is equal to 1 for non-forest vegetation types. Above a specified minimum age, S_{Sag} declines asymptotically to a value of 0.66-0.82, depending on forest type (Turner et al., 2006).

EC-LUE model

Yuan et al. (2007, 2010) developed Eddy Covariance-Light Use efficiency (EC-LUE) model to simulate daily vegetation GPP. The EC-LUE model is driven by only four variables: normalised Difference Vegetation Index (*NDVI*), Photosynthetically Active Radiation (*PAR*), air temperature (*T*), and the Bowen ratio of sensible to latent heat flux.

$$GPP = PAR \times fPAR \times LUE_{\max} \times Min(T_s, W_s) \quad (15)$$

$$fPAR = 1.24 \times NDVI - 0.168 \quad (16)$$

$$T_s = \frac{(T - T_{\min}) \times (T - T_{\max})}{((T - T_{\min}) \times (T - T_{\max}) - (T - T_{opt})^2)} \quad (17)$$

$$W_s = \frac{LE}{R_n} \quad (18)$$

where LUE_{max} is the potential light use efficiency without environmental stress (g C m^{-2} MJ^{-1} APAR). *Min* denotes the minimum values of T_s and W_s, and we assumed that the impacts of temperature and moisture on LUE follow Liebig's Law (i.e., LUE is only affected by the most limiting factor at any given time). T_{min}, T_{max} and T_{opt} are the minimum, maximum and optimum air temperatures (℃) for photosynthetic activity, respectively. If air temperature falls below T_{min} or increases beyond T_{max}, T_s is set to zero. In this study, T_{min} and T_{max} were set to 0 and 40℃,

respectively, while T_{opt} was determined using nonlinear optimisation as 21℃ (Yuan et al., 2007). *LE* is latent heat (MJ m^{-2}), which is estimated by the revised RS-PM (Remote Sensing–Penman Monteith) model (Yuan et al., 2010). R_n is net radiation (MJ m^{-2}).

MODIS-GPP product

MODIS-GPP algorithms (Running et al., 2000) rely heavily on the LUE approach, with inputs from MODIS LAI/fPAR (MOD15A2), land cover, and biome-specific climatologic data sources from NASA's Data Assimilation Office. Light use efficiency is calculated based on two factors: the biome-specific maximum conversion efficiency LUE_{max}, a multiplier that reduces the conversion efficiency when cold temperatures limit plant function, and a second multiplier that reduces the maximum conversion efficiency when vapour pressure deficit (*VPD*) is high enough to inhibit photosynthesis. It is assumed that soil water deficit covaries with *VPD* and that *VPD* will account for drought stress.

$$GPP = PAR \times fPAR \times LUE_{\max} \times T_s \times W_s \tag{19}$$

$$T_s = \begin{cases} 0 & TMIN < TMIN_{\min} \\ \dfrac{TMIN - TMIN_{\min}}{TMIN_{\max} - TMIN_{\min}} & TMIN_{\min} < TMIN < TMIN_{\max} \\ 1 & TMIN > TMIN_{\max} \end{cases} \tag{20}$$

$$W_s = \begin{cases} 0 & VPD > VPD_{\max} \\ \dfrac{VPD_{\min} - VPD}{VPD_{\max} - VPD_{\min}} & VPD_{\min} < VPD < VPD_{\max} \\ 1 & VPD < VPD_{\min} \end{cases} \tag{21}$$

where LUE_{max} is the potential light use efficiency without environmental stress (g C m^{-2} MJ^{-1} APAR). Based on the at-launch landcover product (MOD12), a set of biome-specific radiation use efficiency parameters are extracted from the Biome Properties Look-Up Table (BPLUT) for each

pixel. There are five parameters used to calculate GPP.

VPM model

In the Vegetation Production Model (VPM) (Xiao et al., 2004), the potential *LUE* is affected by temperature, land surface moisture condition and leaf phenology. The following is a brief description of the VPM model:

$$GPP = PAR \times fPAR \times LUE_{\max} \times T_s \times W_s \times P_s \quad (22)$$

In the current version of the VPM model, *fPAR* is assumed to be a linear function of *EVI*, and the coefficient is simply set to be 1.0 (Xiao et al., 2004). T_s, W_s and P_s are the down-regulation scalars for the effects of temperature, water and leaf phenology on the light use efficiency of vegetation, respectively. T_s is estimated at each time step, using the equation developed for the Terrestrial ecosystem Model (Raich et al., 1991) as shown at equation (17).

The VPM also utilizes the *LSWI* (Land Surface Water Index) (Xiao et al., 2004) to help capture effects of water stress and phenology on plant photosynthesis:

$$LSWI = \frac{\rho_{NIR} - \rho_{SWIR}}{\rho_{NIR} + \rho_{SWIR}} \quad (23)$$

where *NIR* refers to the 841–876 nm band, and *SWIR* refers to 1628–1652 nm. Water index was presented as:

$$W_s = \frac{1 + LSWI}{1 + LSWI_{\max}} \quad (24)$$

where $LSWI_{max}$ is the maximum *LSWI* within the plant growing season for individual pixels. P_{scalar} is included to account for the effect of leaf phenology (leaf age) on photosynthesis at the canopy level. In this version of the VPM model, calculation of P_s was dependent upon the longevity of

leaves (deciduous, versus evergreen). For a canopy that was dominated by leaves with a life expectancy of 1 year (one growing season, e.g., deciduous trees), P_s was calculated at two different phases as a linear function of *LSWI* from bud burst to leaf full expansion (phase one) by

$$P_s = \frac{1 + LSWI}{2} \quad (25)$$

After leaf full expansion (phase two), P_s was set to 1, and equation (26) was adopted again during senescence (phase three). The dates for the three phases of phenology (bud burst, full canopy, and senescence) were obtained using an EVI seasonal threshold similar to that of the MODIS phenology product MOD12Q2 (Friedl et al., 2003). Thus for large-scale application of the VPRM across North America, MOD12Q2 dates can be used directly.

VPRM model

Formulation of the VPRM starts from the Vegetation Photosynthesis Model (VPM) of Xiao et al. (2004), which estimates GPP using satellite-based vegetation indices and environmental data, adding a nonlinear function to account for the response of GPP to light. The VPRM can be presented by

$$GPP = PAR \times fPAR \times \frac{1}{(1 + PAR / PAR_0)} \times LUE_{\max} \times T_s \times P_s \times W_s \quad (26)$$

where PAR_0 is the half-saturation value. The other variables were calculated as the VPM models.

References

Friedl, M. A., McIver, D. K., Hodges, J. C. F., Zhang, X. Y., Muchoney, D., Strahler, A. H., Woodcock, C.E., Gopal, S., Schneider, A., Cooper, A., Baccini, A., Gao, F., and Schaaf, C.: Global land cover mapping from MODIS: algorithms and early results, Remote Sensing of

Environment, 83, 287-302, 2002.

King, D. A., Turner, D. P., and Ritts, W. D.: Parameterization of a diagnostic carbon cycle model for continental scale application, Remote Sensing of Environment, 115, 1653-1664, 2011.

Myneni, R. B., and Williams, D. L.: On the relationship between FAPAR and NDVI, Remote Sensing of Environment, 49, 200-211, 1994.

Potter, C. S., Randerson, J. T., Field, C. B., Matson, P. A., Vitousek, P. M., Mooney, H. A., and Klooster, S. A.: Terrestrial ecosystem production: a process model based on global satellite and surface data, Global Biogeochemical Cycles, 74, 811-841, 1993.

Raich, J. W., Rastetter, E. B., Melillo, J. M., Kicklighter, D. W., Steudler, P. A., Peterson, B. J., Grace, A. L., Moore III, B., and Vorosmarty, C. J.: Potential net primary productivity in South America: application of a global model, Ecological Applications, 1, 399-429, 1991.

Running, S. W., Thornton, P. E., Nemani, R., and Glassy, J. M.: Global terrestrial gross and net primary productivity from the Earth Observing System, Methods in ecosystem science, 44-57, 2000.

Turner, D. P., Ritts, W. D., Styles, J. M., Yang, Z., Cohen, W. B., Law, B. E., and Thornton, P. E.: A diagnostic carbon flux model to monitor the effects of disturbance and interannual variation in climate on regional NEP, Tellus B, 585, 476-490, 2006.

Van Tuyl S., Law B. E., Turner D. P., and Gitelman A. I.: Variability in net primary production and carbon storage in biomass across Oregon forests-an assessment integrating data from forest inventories, intensive sites, and remote sensing, Forest Ecology and Management, 209, 273-291, 2005.

Veroustraete, F.: On the use of a simple deciduous forest model for the interpretation of climate

change effects at the level of carbon dynamics, Ecological modeling, 75-76, 221-237, 1994.

Veroustraete, F., Sabbe, H., and Eerens, H.: Estimation of carbon mass fluxes over Europe using the C-Fix model and Euroflux data, Remote Sensing of Environment, 833, 376-399, 2002.

Verstraeten, W. W., Veroustraete, F., and Feyen, J.: On temperature and water limitation of net ecosystem productivity: Implementation in the C-Fix model, Ecological Modelling, 199, 4-22, 2006.

Xiao, X. M., Zhang, Q. Y., Braswell, B., Urbanski, S., Boles, S., Wofsy, S., Moore III, B., and Ojima, D.: Modeling gross primary production of temperate deciduous broadleaf forest using satellite images and climate data, Remote Sensing of Environment, 912, 256-270, 2004.

Yuan, W. P., Liu, S. G., Yu, G. R., Bonnefond, J. M., Chen, J. Q., Davis, K., Desai, A. R., Goldstein, A. H., Gianelle, D., Rossi, F., Suyker, A. E., and Verma, S. B.: Global estimates of evapotranspiration and gross primary production based on MODIS and global meteorology data, Remote Sensing of Environment, 1147, 1416-1431, 2010.

Yuan, W. P., Liu, S. G., Zhou, G. S., Zhou, G. Y., Tieszen, L. L., Baldocchi, D., Bernhofer, C., Gholz, H., Goldstein, A. H., Goulden, M. L., Hollinger, D. Y., Hu, Y., Lawn, B. E., Stoy, P. C., Vesala, T., and Wofsy, S. C.: Deriving a light use efficiency model from eddy covariance flux data for predicting daily gross primary production across biomes, Agricultural and Forest Meteorology, 1433, 189-207, 2007.

211 Table S1. Name, location, and other characteristics of the study sites used in this study.

Vegetation Type	Site	Latitude	Longitude
DBF	Ca-oas	53.63° N	106.20° W
DBF	De-hai	51.08° N	10.45° E
DBF	Dk-sor	55.49° N	11.65° E
DBF	Fr-fon	48.48° N	2.78° E
DBF	Fr-hes	48.67° N	7.06° E
DBF	It-col	41.85° N	13.59° E
DBF	It-non	44.69° N	11.09° E
DBF	It-pt1	45.20° N	9.06° E
DBF	It-ro1	42.41° N	11.93° E
DBF	It-ro2	42.39° N	11.92° E
DBF	It-vig	45.32° N	8.85° E
DBF	Se-abi	68.36° N	18.79° E
DBF	Uk-ham	51.15° N	0.86° W
DBF	Uk-pl3	51.45° N	1.27° W
DBF	Us-bar	44.06° N	71.29° W
DBF	Us-bn2	63.92° N	145.38° W
DBF	Us-dk2	35.97° N	79.10° W
DBF	Us-ha1	42.54° N	72.17° W
DBF	Us-lph	42.54° N	72.18° W
DBF	Us-mms	39.32° N	86.41° W
DBF	Us-moz	38.74° N	92.20° W
DBF	Us-umb	45.56° N	84.71° W
DBF	Us-wcr	45.81° N	90.08° W
DBF	Us-wi1	46.73° N	91.23° W
DBF	Us-wi8	46.72° N	91.25° W
EBF	Au-tum	35.66° S	148.15° E
EBF	Au-wac	37.43° S	145.19° E
EBF	Br-ban	9.82° S	50.16° W
EBF	Br-ma2	2.61° S	60.21° W
EBF	Br-sa1	2.86° S	54.96° W
EBF	Cn-bed	39.53° N	116.25° E
EBF	Cn-ku1	40.54° N	108.69° E
EBF	Fr-pue	43.74° N	3.60° E
EBF	Gf-guy	5.28° N	52.93° W
EBF	Id-pag	2.35° N	114.04° E
EBF	It-cpz	41.71° N	12.38° E
EBF	It-lec	43.30° N	11.27° E
EBF	Pt-mi1	38.54° N	8.00° W
EBF	Vu-coc	15.44° S	167.19° E
ENF	Ca-ca1	49.87° N	125.33° W

ENF	Ca-ca2	49.87° N	125.29° W
ENF	Ca-ca3	49.53° N	124.90° W
ENF	Ca-man	55.88° N	98.48° W
ENF	Ca-ns1	55.88° N	98.48° W
ENF	Ca-ns2	55.91° N	98.52° W
ENF	Ca-ns3	55.91° N	98.38° W
ENF	Ca-ns4	55.91° N	98.38° W
ENF	Ca-ns5	55.86° N	98.49° W
ENF	Ca-obs	53.99° N	105.12° W
ENF	Ca-ojp	53.92° N	104.69° W
ENF	Ca-qcu	49.27° N	74.04° W
ENF	Ca-qfo	49.69° N	74.34° W
ENF	Ca-sf1	54.49° N	105.82° W
ENF	Ca-sf2	54.25° N	105.88° W
ENF	Ca-sj1	53.91° N	104.66° W
ENF	Ca-sj2	53.94° N	104.65° W
ENF	Ca-sj3	53.88° N	104.64° W
ENF	Ca-tp1	42.66° N	80.56° W
ENF	Ca-tp2	42.77° N	80.46° W
ENF	Ca-tp3	42.71° N	80.35° W
ENF	Ca-tp4	42.71° N	80.36° W
ENF	Cz-bk1	49.50° N	18.54° E
ENF	De-har	47.93° N	7.60° E
ENF	De-tha	50.96° N	13.57° E
ENF	De-wet	50.45° N	11.46° E
ENF	Es-es1	39.35° N	0.32° W
ENF	Fi-hyy	61.85° N	24.29° E
ENF	Fi-sod	67.36° N	26.64° E
ENF	Fr-lbr	44.72° N	0.77° W
ENF	Il-yat	31.34° N	35.05° E
ENF	It-lav	45.96° N	11.28° E
ENF	It-ren	46.59° N	11.43° E
ENF	It-sro	43.73° N	10.28° E
ENF	Nl-loo	52.17° N	5.74° E
ENF	Ru-fyo	56.46° N	32.92° E
ENF	Ru-zot	60.80° N	89.35° E
ENF	Se-fla	64.11° N	19.46° E
ENF	Se-nor	60.09° N	17.48° E
ENF	Se-sk1	60.13° N	17.92° E
ENF	Se-sk2	60.13° N	17.84° E
ENF	Sk-tat	49.12° N	20.16° E
ENF	Uk-gri	56.61° N	3.80° W
ENF	Us-blo	38.90° N	120.63° W

ENF	Us-dk3	35.98° N	79.09° W
ENF	Us-fmf	35.14° N	111.73° W
ENF	Us-fuf	35.09° N	111.76° W
ENF	Us-ho1	45.20° N	68.74° W
ENF	Us-ks1	28.46° N	80.67° W
ENF	Us-me1	44.58° N	121.50° W
ENF	Us-me2	44.45° N	121.56° W
ENF	Us-me3	44.32° N	121.61° W
ENF	Us-me4	44.50° N	121.62° W
ENF	Us-nc2	35.80° N	76.67° W
ENF	Us-nr1	40.03° N	105.55° W
ENF	Us-sp2	29.76° N	82.24° W
ENF	Us-sp3	29.75° N	82.16° W
ENF	Us-wi2	46.69° N	91.15° W
ENF	Us-wi4	46.74° N	91.17° W
ENF	Us-wi5	46.65° N	91.09° W
ENF	Us-wi9	46.62° N	91.08° W
ENF	Us-wrc	45.82° N	121.95° W
GRA	At-neu	47.12° N	11.32° E
GRA	Ca-let	49.71° N	112.94° W
GRA	Ch-oe1	47.29° N	7.73° E
GRA	Cn-du2	42.05° N	116.28° E
GRA	Cn-ham	37.37° N	101.18° E
GRA	Cn-xi1	43.55° N	116.68° E
GRA	Cn-xi2	43.55° N	116.67° E
GRA	Cz-bk2	49.50° N	18.54° E
GRA	De-gri	50.95° N	13.51° E
GRA	De-meh	51.28° N	10.66° E
GRA	Dk-lva	55.68° N	12.08° E
GRA	Es-vda	42.15° N	1.45° E
GRA	Fi-sii	61.83° N	24.19° E
GRA	Fr-lq1	45.64° N	2.74° E
GRA	Fr-lq2	45.64° N	2.74° E
GRA	Hu-bug	46.69° N	19.60° E
GRA	Hu-mat	47.85° N	19.73° E
GRA	Ie-dri	51.99° N	8.75° W
GRA	It-amp	41.90° N	13.61° E
GRA	It-be2	46.00° N	13.03° E
GRA	It-mal	46.12° N	11.70° E
GRA	It-mbo	46.02° N	11.05° E
GRA	Nl-ca1	51.97° N	4.93° E
GRA	Nl-hor	52.03° N	5.07° E
GRA	Pt-mi2	38.48° N	8.02° W

GRA	Ru-ha2	54.77° N	89.96° E
GRA	Ru-ha3	54.70° N	89.08° E
GRA	Uk-ebu	55.87° N	3.21° W
GRA	Us-arb	35.55° N	98.04° W
GRA	Us-arc	35.55° N	98.04° W
GRA	Us-aud	31.59° N	110.51° W
GRA	Us-bkg	44.35° N	96.84° W
GRA	Us-cav	39.06° N	79.42° W
GRA	Us-dk1	35.97° N	79.09° W
GRA	Us-fwf	35.45° N	111.77° W
GRA	Us-goo	34.25° N	89.87° W
GRA	Us-ib2	41.84° N	88.24° W
GRA	Us-var	38.41° N	120.95° W
GRA	Us-wkg	31.74° N	109.94° W
GRA	Ru-che	68.61° N	161.34° E
MF	Be-bra	51.31° N	4.52° E
MF	Be-jal	50.56° N	6.07° E
MF	Be-vie	50.31° N	6.00° E
MF	Ca-gro	48.22° N	82.16° W
MF	Cn-cha	42.40° N	128.10° E
MF	Jp-tef	45.06° N	142.11° E
MF	Jp-tom	42.74° N	141.51° E
MF	Us-pfa	45.95° N	90.27° W
MF	Us-syv	46.24° N	89.35° W

212 DBF: deciduous broadleaf forest; EBF: evergreen broadleaf forest; ENF: evergreen needleleaf

213 forest; GRA: grassland; MF: mixed forest.

214

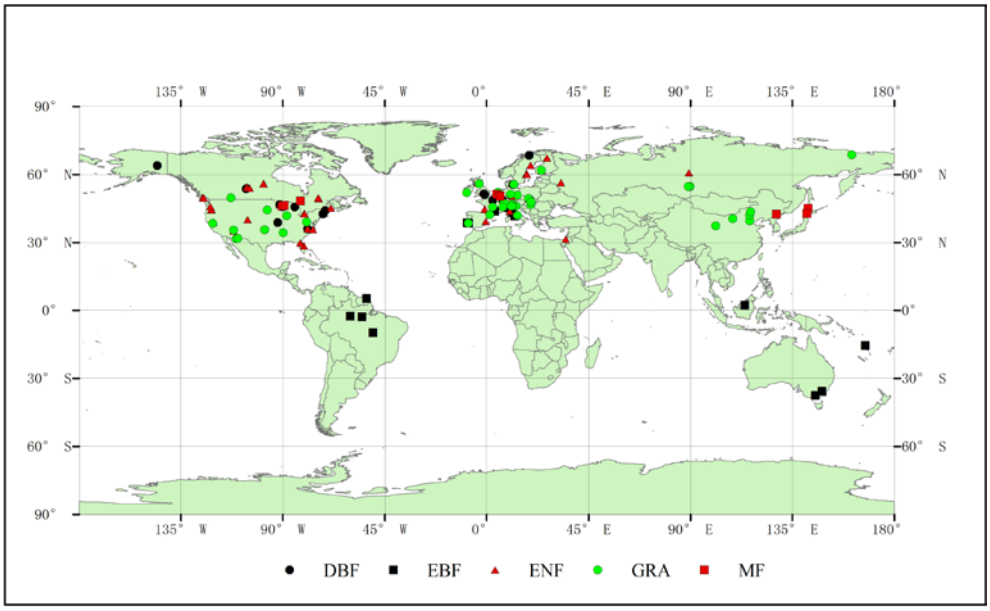

Figure S1. The location of sites in this study. DBF: deciduous broadleaf forest; EBF: evergreen broadleaf forest; ENF: evergreen needleleaf forest; GRA: Grassland; MF: Mixed forest.